JOURNAL OF CATALYSIS **161,** 694–703 (1996)
ARTICLE NO. 0231

Interaction of Sulfate Groups with the Surface of Zirconia: An HRTEM Characterization Study

M. Benaïssa, J. G. Santiesteban,*[,1] G. Díaz, C. D. Chang,* and M. José-Yacamán

*Instituto de Física, Universidad Nacional Autónoma de México, A.P. 20-364, México D.F. 01000, Mexico; and *Mobil Research and Development Corp., Central Research Laboratory, Princeton, New Jersey 08540*

Received October 24, 1995; revised March 12, 1996; accepted March 25, 1996

High-resolution transmission electron microscopy (HRTEM) has been used to characterize the morphology and the surface structure at an atomic level of sulfated zirconia and sulfate-free zirconia. Our study shows that HRTEM can be used to directly observe sulfate layers adsorbed on the surface of zirconia crystallites. The results indicate that the presence of sulfate groups not only stabilizes the tetragonal zirconia phase, but also induces the formation of well-faceted small zirconia crystallites. In particular, it is observed that the presence of sulfate groups induces the preferential formation of relatively long-flat (110) plane of tetragonal zirconia. HRTEM images of this plane revealed the presence of an adsorbed sulfate layer. It is proposed that the geometry of the (110) plane is such that it can accommodate sulfate groups in a two- or threefold coordination. Although, zirconia crystallites with relatively long-flat {110} planes containing adsorbed sulfate groups were clearly predominant in the sulfated zirconia catalyst; its role in the formation of the highly acidic sites is not clear. Our study also reveals the presence of few zirconia crystallites containing rough surfaces, crystallographically speaking high-Miller-index surfaces, which if they were to contain sulfate groups, they could be the locus of the highly acidic sites. Thus, it is suggested that caution must be taken when performing spectroscopic studies using techniques such as IR, NMR, XPS, and Raman to distinguish between spectator sulfate groups, which could be a majority if they were the ones observed on the (110) plane, and those participating in the formation of the highly acidic site, which could be associated to the few high-Miller-index-containing zirconia crystallites.

1. INTRODUCTION

In the past few years, sulfated zirconia catalyst has been reported to be the most promising solid acid candidate to replace liquid acids and halogen-containing solid acids, which are highly corrosive and are subject to stringent environmental regulations. The high acid activity of the sulfated zirconia catalyst, referred to by some researchers as superacid activity (1, 2), facilitates paraffin isomerization reactions under conditions much milder, near room temperature, then those used with conventional solid acid catalysts, for example, zeolites. Despite extensive characterization studies using a great variety of spectroscopic techniques (3–12), the nature and structure of the highly acidic sites on SO_4^{2-}/ZrO_2 are still a matter of controversy. An understanding of the nature of the highly acidic sites could be reached by a good knowledge of the factors which control the surface structure of the catalyst. High-resolution transmission electron microscopy (HRTEM) is a powerful tool which can provide direct images of a projected structure of individual metallic particles and/or oxide surfaces (13–16). In the present study, information at an atomic level on local surfaces of sulfate-free zirconia and sulfated zirconia particles has been obtained using HRTEM imaging. Our approach consisted of aligning the crystallite surface of interest parallel to the electron beam. This allows one to record atomic detail of both the bulk and the one-dimensional projection of the structure of the crystallite edge. Elucidation of the structure of the crystallite edge, which is interpreted in terms of the crystallite surface, may yield atomic-scale information on the surface structure. HRTEM images have been recorded around Scherzer defocus, so that every dark spot corresponds to a single atomic column and/or assembly of atomic columns. This has the advantage of avoiding Fresnel-like oscillations obtained when working at white contrast defocus, which generally confuses surface details.

The HRTEM images presented in this study are devoted to help in understanding the correlation between surface structure, which governs the nature of electronic surface states, and the high acid activity exhibited by the sulfated zirconia catalyst.

2. EXPERIMENTAL PROCEDURE

2.1. Materials

Sulfated zirconia, SO_4^{2-}/ZrO_2, was prepared by using a two-step procedure. First, $Zr(OH)_4$ was synthesized by

[1] To whom correspondence should be addressed at current address: Air Products and Chemicals, Inc., 7201 Hamilton Boulevard, Allentown, PA 18195-1501. Fax: (610) 418-7719.

0021-9517/96 $18.00

precipitating a zirconyl nitrate ($ZrO(NO_3)_2$) solution with an aqueous NH_4OH solution (28% NH_3). The precipitated gel, $Zr(OH)_4$, was washed thoroughly with deionized water, filtered, and air dried at 383 K for 14 h. In the second step, the dried $Zr(OH)_4$ was impregnated with a 1 N aqueous solution of $(NH_4)_2SO_4$. The resulting slurry was dried at 383 K for 14 h, followed by dry air calcination at 998 K for 1 h. Sulfur content, as determined by chemical analysis, was 1.33 wt%, which corresponds to 4.0 wt% SO_4^{2-}. The BET surface area was 90 m^2/g. The estimated surface concentration of sulfate groups, assuming a diameter for the SO_4^{2-} anion of 0.58 nm, is 2.9 SO_4^{2-}/nm^2, or approximately half a monolayer in terms of overall surface coverage. It has been reported that at this surface density, SO_4^{2-} groups exist as a mixture of isolated sulfates and complex polynuclear sulfates (5).

Two sulfate-free ZrO_2 samples were also prepared for comparison purposes. They were prepared by calcining $Zr(OH)_4$, which was prepared according to the above procedure, at two different temperatures, 773 and 998 K. These samples are designated in the text and figures as $ZrO_{2(773)}$ and $ZrO_{2(998)}$, and their BET surface areas were 90 and 25 m^2/g, respectively.

2.2. *High-Resolution Transmission Electron Microscopy*

HRTEM was carried out using a JEM4000EX electron microscope operated at 400 keV. Electron micrographs were recorded at magnification of 600,000×. Samples were supported on holey carbon-coated copper grids by simply grinding the specimen between two glass plates and bringing the powder into contact with the grid. All images were recorded on particles which protruded over openings in the carbon support of the copper grids.

Powder X-ray diffraction analyses were also carried out for phase identification of the sample.

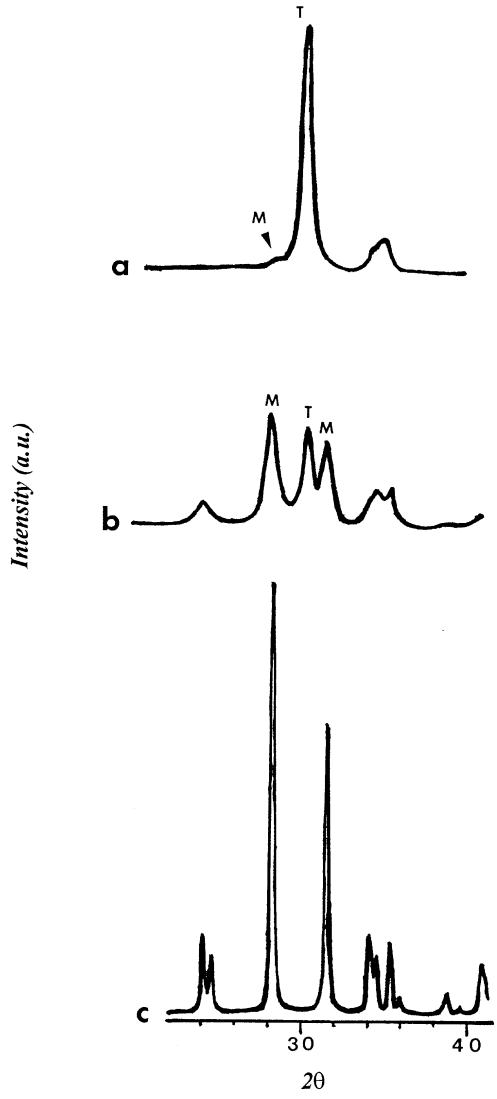

FIG. 1. X-ray diffraction patterns of (a) sulfated zirconia calcined at 998 K, (b) sulfate-free zirconia calcined at 773 K, $ZrO_{2(773)}$, and (c) sulfate-free zirconia calcined at 998 K, $ZrO_{2(998)}$.

3. RESULTS AND DISCUSSION

3.1. *Particle Size, Morphology, and Crystal Structure*

XRD pattern of the SO_4^{2-}/ZrO_2 sample, Fig. 1a, indicates that the crystalline form of ZrO_2 is mainly tetragonal. An aditional small peak that appears at the angle $2\theta = 28.2^\circ$ may be interpreted as a presence of monoclinic zirconia traces.

Figures 1b and 1c show the XRD patterns of sulfate-free ZrO_2 samples calcined at 773 and 998 K, respectively. These XRD patterns reveal that a mixture of tetragonal and monoclinic phases is present in the $ZrO_{2(773)}$ material, Fig. 1b, while the $ZrO_{2(998)}$ material contains solely the monoclinic phase. In addition, the sharp XRD peaks exhibited by the $ZrO_{2(998)}$ material indicate that a significant sintering, which gives rise to large crystallite sizes, took place during the high-temperature calcination.

It is apparent from these XRD results, and the results of authors (2, 17), that the presence of SO_4^{2-} stabilizes the metastable tetragonal ZrO_2 and retards the sintering process. The stabilization of the metastable tetragonal ZrO_2 has also been reported to take place with the incorporation of many different metal oxides such as MgO, CaO, Sc_2O_3, Y_2O_3, La_2O_3, and CeO_2, and the mechanism governing the process of stabilization is still not fully understood (18). Although it is generally accepted that the tetragonal phase is present in the highly acidic SO_4^{2-}/ZrO_2 catalysts, it is not clear if it plays any direct role in the formation of the highly acidic sites present in this material.

Now, let us discuss the morphology and particle size of the ZrO_2 samples. Figure 2a shows a typical region of the

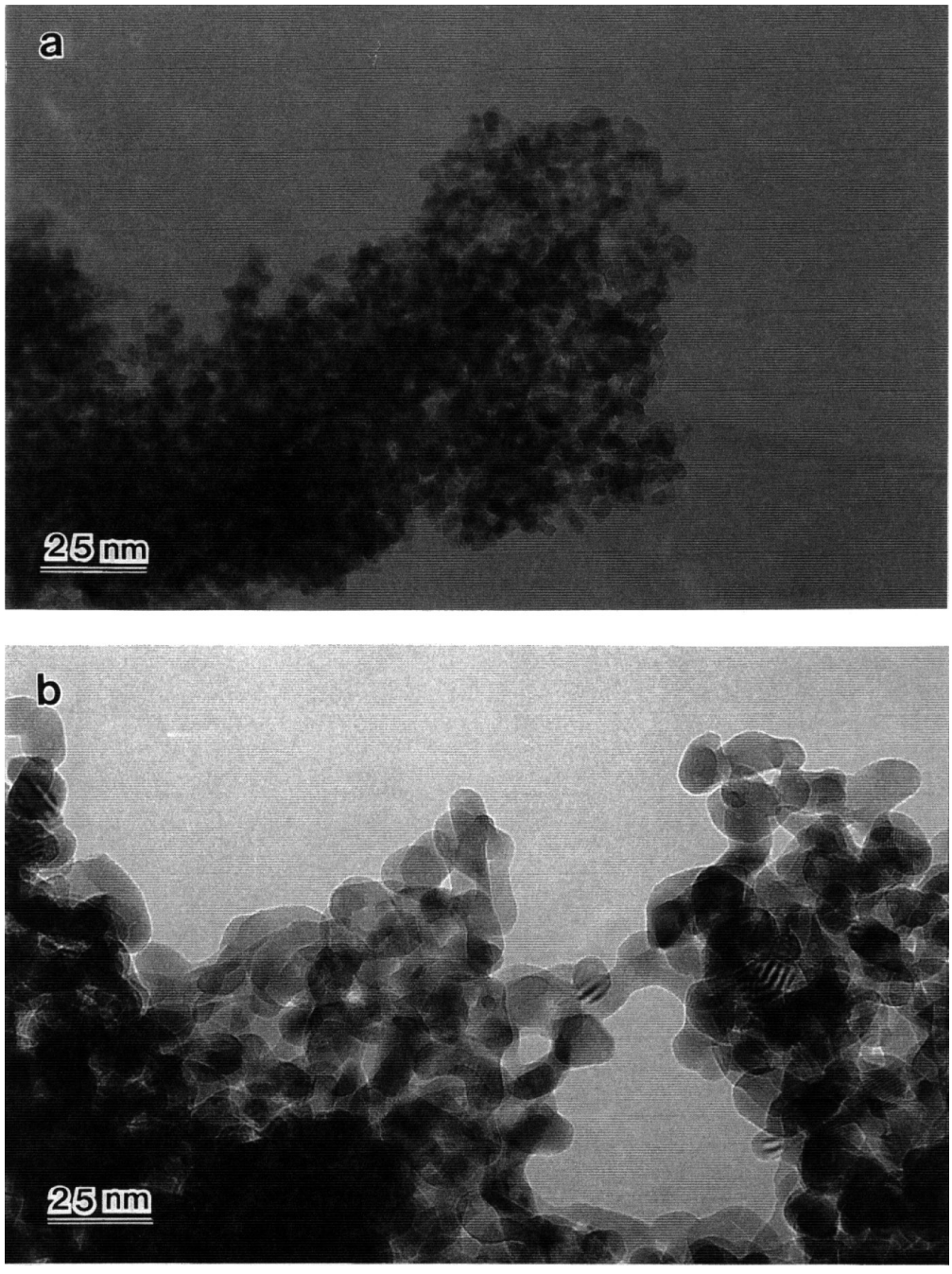

FIG. 2. Typical low-magnification electron micrographs for (a) sulfated zirconia calcined at 998 K, (b) sulfate-free zirconia calcined at 773 K, $ZrO_{2(773)}$, and (c) sulfate-free zirconia calcined at 998 K, $ZrO_{2(998)}$.

sulfated ZrO_2. The average particle size of this material remains relatively small, <10 nm, despite the high calcination temperature, 998 K, used in its preparation. The most striking feature of the sulfated ZrO_2 is the abundance of faceted particles. This result indicates that the SO_4^{2-} groups not only retard the sintering process of the tetragonal ZrO_2 crystallites but also decrease to a great extent their defective terminations.

Typical low-magnification electron micrographs of the sulfate-free ZrO_2 materials, $ZrO_{2(773)}$ and $ZrO_{2(998)}$, are presented in Figs. 2b and 2c. The particle size in the case of $ZrO_{2(773)}$, Fig. 2b, is in the 10 nm range, and their shape is more or less rounded, indicating defective (or stepped) terminations. Considerable sintering, as also revealed by XRD, is observed in the high-calcination temperature sulfate-free $ZrO_{2(998)}$ sample, Fig. 2c. Its average particle size is >20 nm.

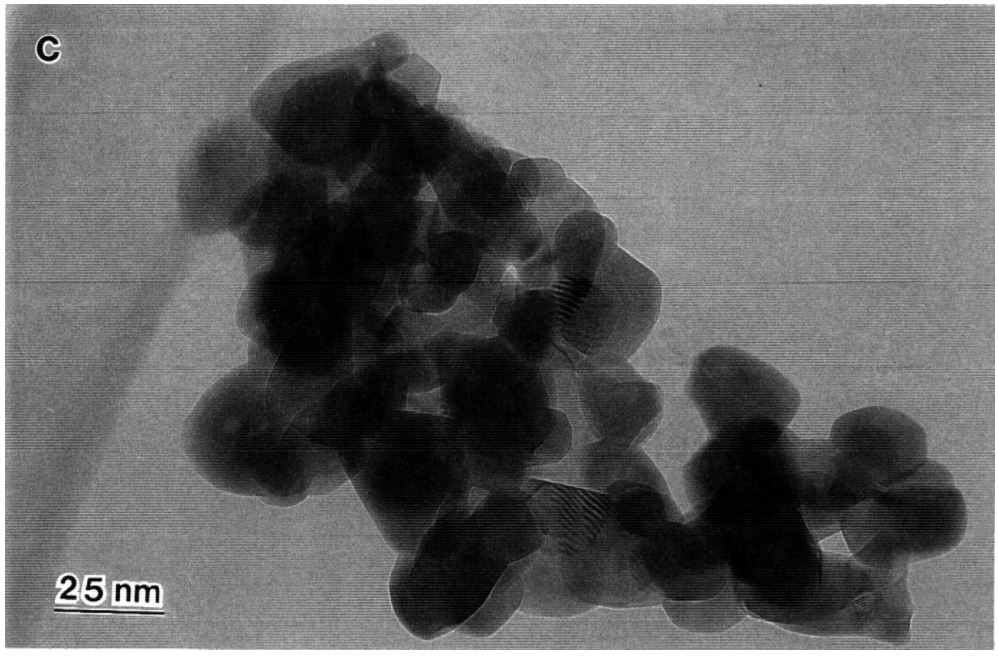

FIG. 2—*Continued*

3.2. Surface Atomic Structure

In this section, we compare the surface atomic structure of the sulfated ZrO_2, material calcined at 998 K, with that of the sulfate-free $ZrO_{2(773)}$, calcined at 773 K. Only the tetragonal ZrO_2 particles of the former are discussed, as this is the phase present in the sulfated ZrO_2 catalyst.

3.2.a. $ZrO_{2(773)}$. Typical high-resolution TEM micrographs of crystallites observed in the $ZrO_{2(773)}$ material are shown in Figs. 3 and 4. Two crystallographic orientations were frequently observed; namely ⟨111⟩ (Fig. 3) and ⟨010⟩ (Fig. 4). The zirconia crystallite surfaces are free of contamination so that their surface morphology can be characterized at the atomic level. Along the ⟨111⟩ orientation, Fig. 3, long {101} plane terminations are clearly visible, together with some short {011} surface planes that give rise to surface atomic steps. Similarly, many monoatomic steps can be identified from the HRTEM zirconia image along the ⟨010⟩ orientation in Fig. 4. Along this orientation, the {101} faces do not show long plane terminations. This can probably be related to the crystallite size. The energetically stable configuration of the zirconia crystallite and the substantial rearrangement of the crystallite profile are likely to be sensitive either to the crystallite size or to the adsorption of foreign species, or both. Since the images show very clean zirconia surfaces, the crystallite surface configuration in Fig. 4 is then due to the size effect. This result leads us to conclude that there is a critical crystallite size ($\leq$5 nm) in the sulfate-free ZrO_2 under which the appearance of many one-atom-height steps is favored. Above this crystallite size the number of surface steps is considerably reduced.

Surface defects are of great interest to catalysis since they contain low-coordination number atoms with coordinatively unsaturated bonds ready to serve as adsorption sites. Therefore, one could argue that the defects observed on the sulfate-free zirconia crystallites are seats of acid activity; however, the acid strength of these sites must be too weak since pure ZrO_2 does not catalyze reactions that demand relatively strong acid sties, such as butane isomerization.

3.2.b. Sulfated zirconia. As in the case of the sulfate-free zirconia, the ⟨010⟩ and ⟨111⟩ orientations were also clearly predominant in the sulfate-modified material. A HRTEM image of a sulfated zirconia crystallite along the ⟨010⟩ orientation is presented in Fig. 5. The contrast exhibited in this image is similar to that of Fig. 4, although here a slight disorientation with respect to the electron beam axis means that the fringes run preferably in one direction. The crystallite of Fig. 5 shows a faceted shape exhibiting two kind of faces; namely regular {101} and {001} faces and slightly rough {100} face. This surface roughness can also be interpreted in terms of surface atomic steps. Crystallographically speaking, the combination of these surface atomic steps gives rise to surfaces of high Miller index, which from an energetic point of view produce very favorable adsorption sites (19). It would be appealing to propose that the presence of sulfate groups near or on these high-Miller-index surfaces could give rise to the highly acidic sites of sulfated zirconia. The presence of sulfate groups on those particles is very likely, as the proven effect of the presence of sulfate is the stabilization of tetragonal zirconia

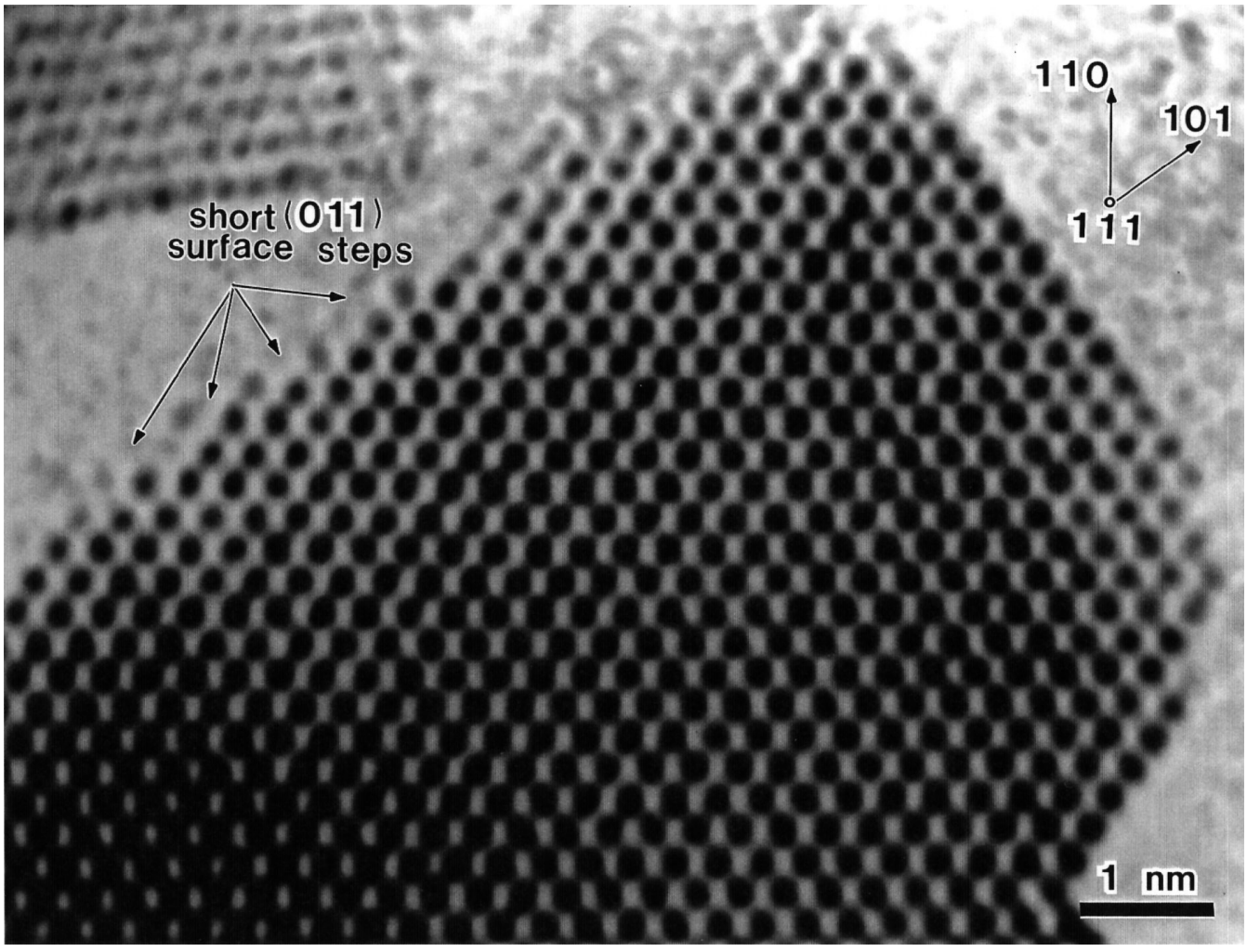

FIG. 3. HRTEM micrograph for sulfate-free zirconia calcined at 773 K, $ZrO_{2(773)}$, along the ⟨111⟩ crystallographic orientation. Note the presence of short surface atomic steps.

particles at the high calcination temperature used in this study (998 K). However, the presence of sulfate groups on these high-Miller-index short surfaces was not apparent from our study due to the limitations of the HRTEM technique. A rough surface is a 3D object, while the edge of the particle provided by a micrograph is only 1D, so details on the rough surfaces are lost during transmission electron microscopy studies. It is also important to mention that the number of ZrO_2 crystallites that have "rough surfaces" or high Miller indices is very small compared to the particles that have flat or regular surfaces that are discussed below. These results imply that the number of highly acidic sites on the sulfated zirconia would be low if they were present on these small highly defective particles.

HRTEM images of sulfated zirconia along the ⟨111⟩ orientation are shown in Figs. 6a and 6b. In these images, we can recognize the periodicity already observed in the HRTEM images of sulfate-free zirconia (Fig. 3). As it was mentioned above, the sulfated zirconia particles have a markedly faceted shape; with the {110} plane terminations being clearly predominant. The {110} faces do not exhibit apparent monoatomic steps, as was the case on the {110} faces present on the sulfate-free zirconia particles (see Fig. 3). It is proposed that the faceted shape of the relatively small zirconia crystallites in the sulfate-containing material results from both the presence of sulfate and the thermal effect. The latter is indeed enhancing the formation of the most stable faces, while the presence of sulfate is favoring the formation of small particles of the tetragonal zirconia phase.

While the HRTEM image along the ⟨010⟩ orientation, Fig. 5, does not show any extra surface features, the HRTEM images in Figs. 6a and 6b show surface details in the form of quasi-continuous line of repeated dark spots along the {110} top atomic layer. Careful examination shows that the top layer contrast is quite different from the

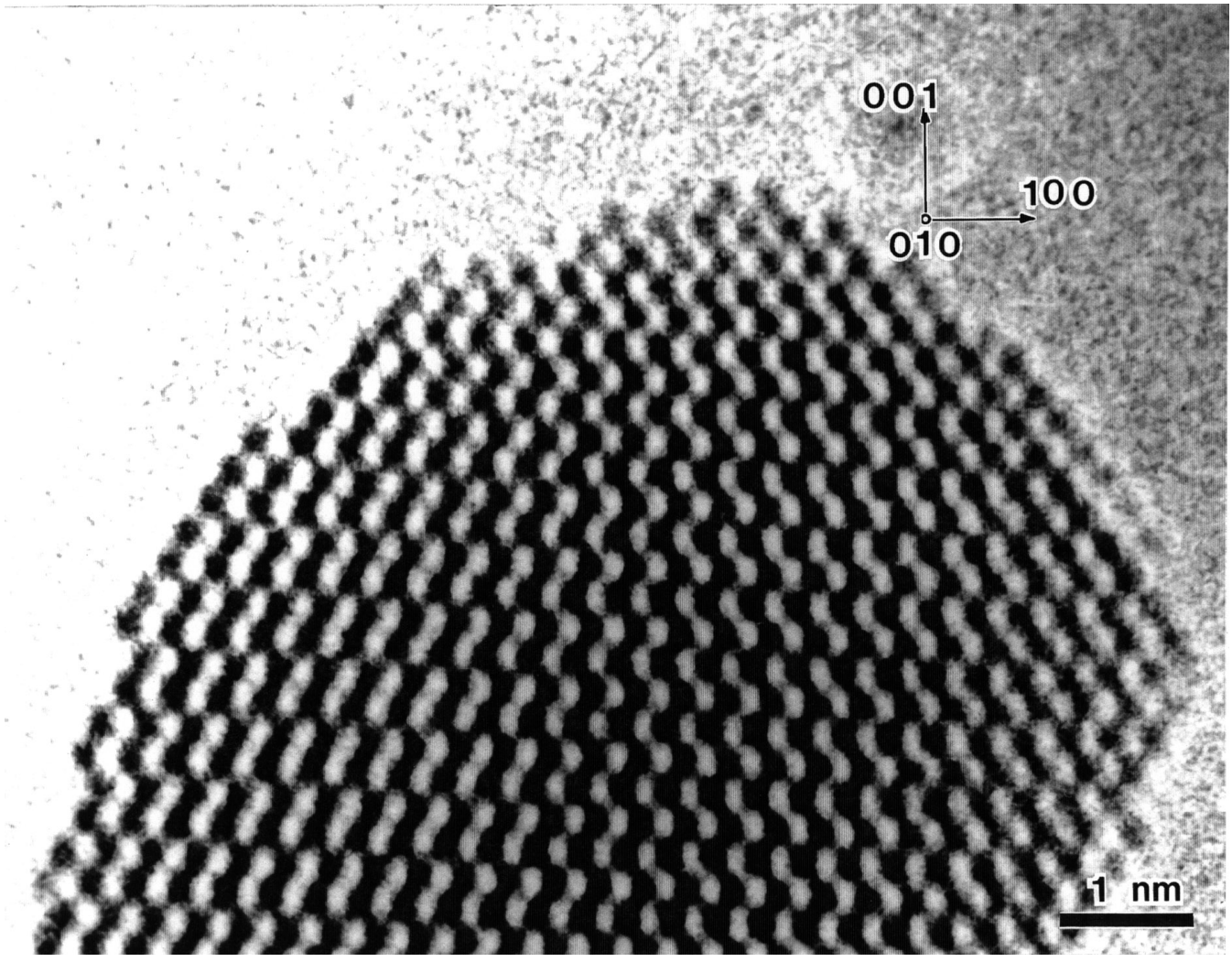

FIG. 4. HRTEM micrograph for sulfate-free zirconia calcined at 773 K, $ZrO_{2(773)}$, along the ⟨010⟩ crystallographic orientation. Note the abundance of defective terminations.

immediate underneath layers. These surface features were visible over a limited range of defoci (around Scherzer) recorded experimentally *(the focus difference between images in Figs. 6a and 6b, respectively, is on the order of 10 nm)*. This slight variation in defocus makes the detection of the variable atomic occupancy on the surface unmistakable. The variation of the defocus clearly shows surface vacancies located on the top layer of the particle. Moreover, the image of Fig. 6b exhibits white fringes having a periodicity of 0.515 nm, equal to the double of the ZrO_2 (110) plane distance. If we follow the white-fringe periodicity perpendicularly from the bulk toward the edge, the white line terminates exactly at the top layer. This contrast periodicity was not visible in the sulfate-free zirconia samples and would be difficult to explain based on surface roughness or anion vacancies. The observed surface features in Figs. 6a and 6b can be explained by the formation of a sulfate complex layer. The presence of sulfate groups on this sample is evidenced by the stabilization of the metastable tetragonal zirconia. As discussed in Section 3.1, sulfate-free zirconia calcined at 998 K, which is the same calcination temperature used for the preparation of the sulfated zirconia sample, contains solely monoclinic zirconia phase. In addition, it was clear from our observations that the presence of sulfate groups induces (110) faceting of the tetragonal zirconia crystallites. The question regarding the image of Fig. 6 is whether a sulfate complex layer could be evidenced by the phase contrast, and the answer is yes. Image simulations have recently demonstrated (20, 21) that an adsorbed sulfur overlayer on a Pt particle produces sufficient contrast to be observed by HRTEM.

Let us go back to the image of Fig. 6, and try to extract information about the possible sulfate groups location upon the zirconia surface. The spacing between two

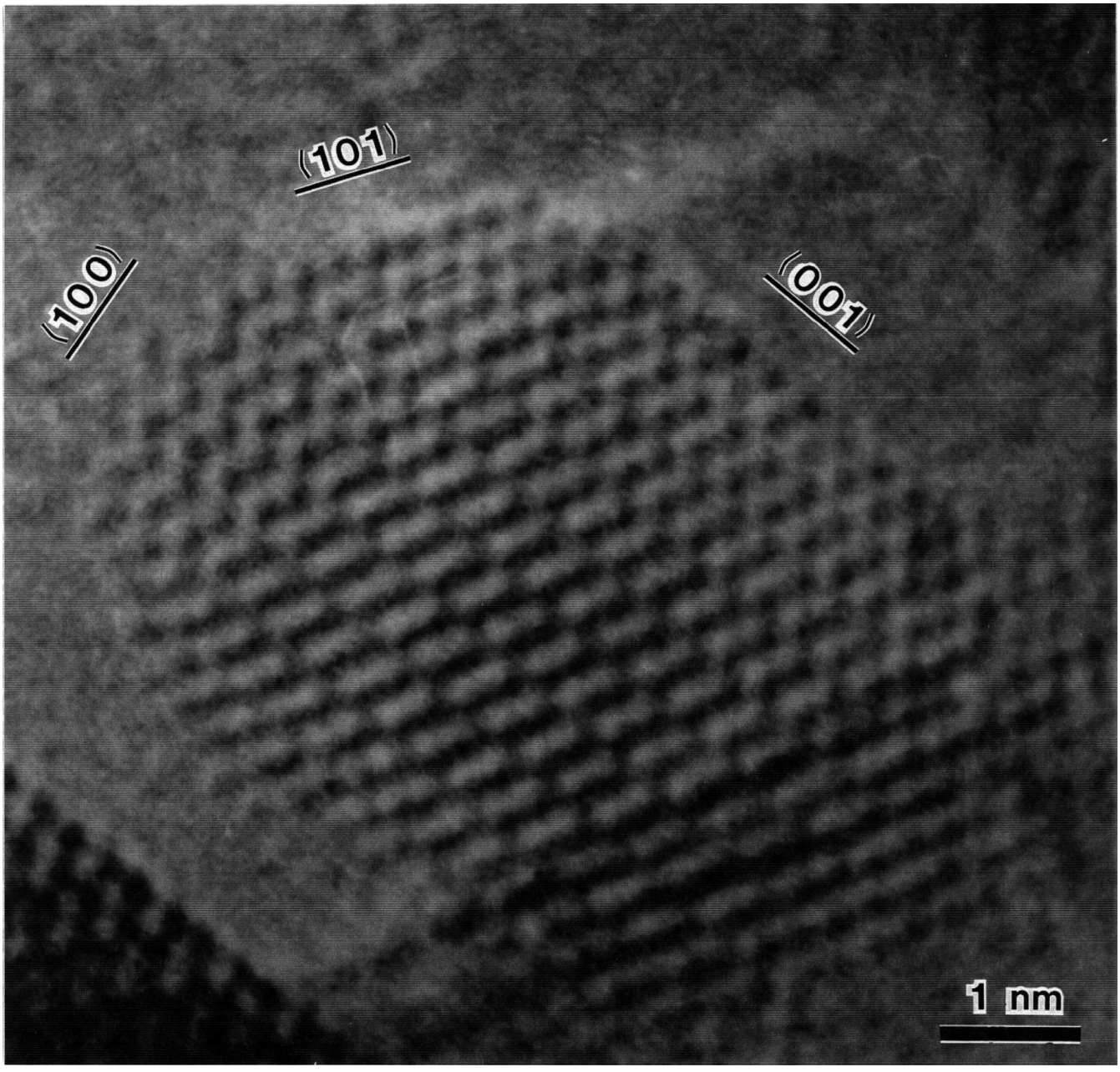

FIG. 5. HRTEM micrograph for sulfated zirconia calcined at 998 K along the ⟨010⟩ crystallographic orientation. A faceted particle showing two kind of surface terminations namely regular {101} and {001} faces and a slightly rough {100} face.

dark spots along the (110) plane is equal to 0.368 nm. Compared to the extra-top-layer periodicity, we notice that the dark spots along the adsorbed layer have exactly the same periodicity, but the spots are shifted by 0.184 nm, which is half the spacing along the (110) plane. This result indicates that the sulfate groups are located between Zr atoms. The side view image of the (110) plane cannot distinguish whether the sulfate group is bridging across two or three zirconium atoms, as depicted by the top view of the (110) plane in Figs. 7a and 7b. Both sulfate structures have been proposed to exist on the ZrO_2 surface. For example, Riemer *et al*. (11) carried out Raman and MAS NMR studies, and proposed a sulfate structure, suggested earlier by Bensitel *et al*. (5), that consists of a single S=O double bond with the sulfur atom anchored to the oxide surface through three S–O–Zr linkages, as shown in Fig. 7a. In contrast, several researchers (10) support Tanabe's earlier bidenatate structure (2), which consisted on two S=O double bonds with the sulfur atom anchored to the oxide surface through two S–O–Zr linkages, as shown in Fig. 7b.

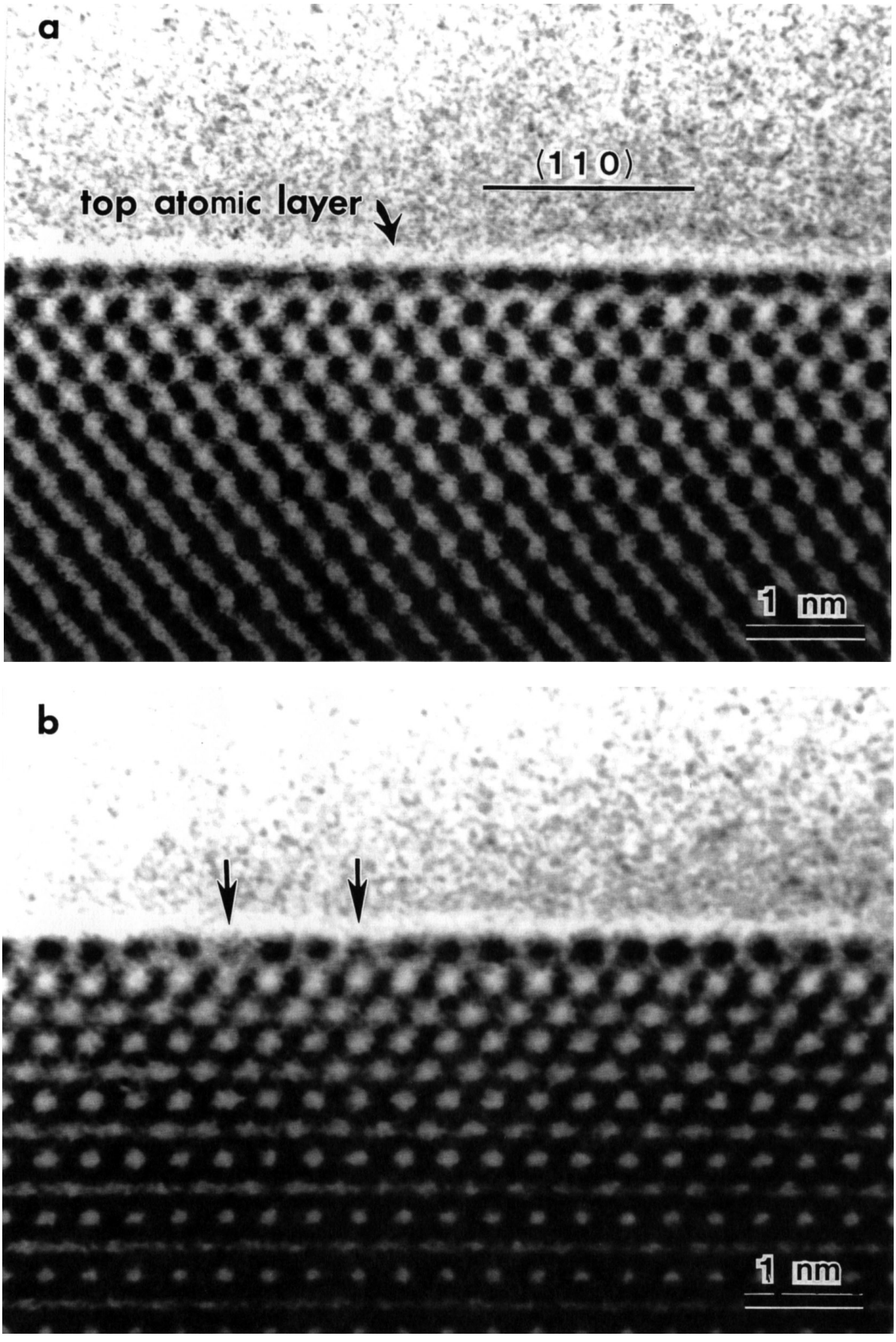

FIG. 6. HRTEM micrograph for sulfated zirconia calcined at 998 K along the ⟨111⟩ crystallographic orientation. (a) and (b) are images of the same particle but with a slight different defocus to show surface features. Note in (b) the appearance of some vacancies (arrows) at the top-layer and white fringes having a periodicity equal to the double of that of (110) planes.

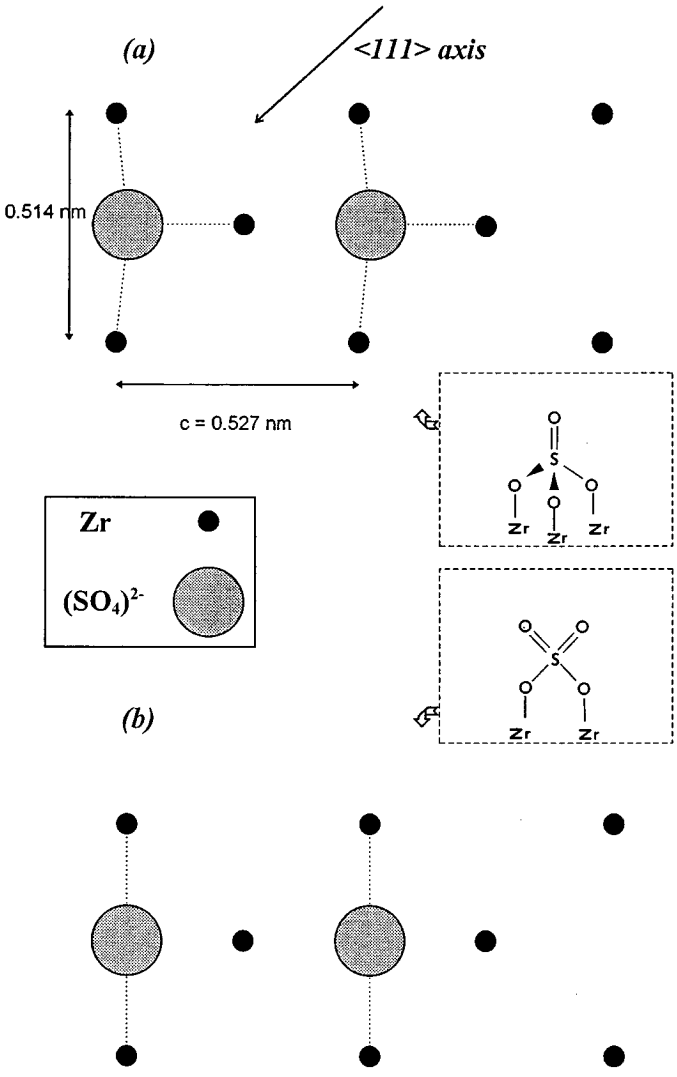

FIG. 7. Top view of proposed structures of adsorbed sulfate groups on the (110) plane of zirconia. (a) Threefold coordination and (b) twofold coordination.

To construct a model of adsorbate sulfates which accounts for the observed HRTEM image contrast, we must at least take into account a compatible arrangement with existing surface studies on model crystals. Unfortunately, the lack of studies regarding zirconia single crystals loaded with sulfates makes the prediction of a reasonable model not straightforward. An example is given by early studies on the morphological changes of platinum particles occurring upon sulfiding (15). While extensive modeling and image calculations have led to a refined model of a sulfur monolayer on a cubic platinum particle which match very well with HRTEM surface images (20), other investigations using the same sample and the same model showed many difficulties in reconciling using the same sample and the same model showed many difficulties in reconciling the transmitted contrast of simulated images with the surface imaging contrast (21), even if low-energy electron diffraction (LEED) data were available in the literature. In this context, it should be mentioned that the adsorption sites of sulfate on any surface of zirconia are not precisely known. While extensive image simulations have been obtained, the agreement with our experimental images is still uncertain. Although the periodicity of surface features observed in the HRTEM images will not change by inverting the structures, agreement with experiments is not easily obtained mainly because of two factors; (i) the difference in the scattering factors of Zr, O, and S, and (ii) the lack of the exact distribution of the *interatomic distances* and *coordination numbers* of the different atoms involved along the surface and within the three to four zirconia top layers.

4. CONCLUSIONS

Our HRTEM study provided information at an atomic level on the sulfated zirconia surface configuration. We demonstrated the potential of HRTEM to directly observe sulfate surface complexes on sulfated zirconia catalysts. This capability combined with other characterization techniques and catalytic measurements should prove useful in elucidating the structure and/or nature of the highly acidic sites present on the sulfated zirconia material.

Specifically, the following conclusions can be drawn from our study:

(1) The presence of SO_4^{2-} groups not only stabilizes small tetragonal ZrO_2 crystallites, but also induces the formation of well-faceted particles, i.e., decreases the number of defective terminations.

(2) The shape of the sulfated zirconia crystallites exhibits two types of surfaces: long-smooth and a relatively few short-rough planes. With the long-smooth (110) plane being clearly predominant.

(3) Comparison between sulfate-free and sulfated zirconia materials indicates that the presence of SO_4^{2-} induces the (110) faceting of the zirconia particles. A layer of isolated sulfate groups has been directly observed on the long-flat (110) surface of the zirconia. The geometry of this plane is such that it can accommodate the sulfate groups in a two- or threefold coordination, i.e., bidentate or tridentate structure. The HRTEM image contrast cannot distinguish between these two structures. It is not clear whether the observed sulfate groups on the presumably defect-free (110) plane play any role in the formation of the highly acidic site or they are just "spectators." This could mask information on the actual acid sites, which could be present on the particles described below. Thus, it is suggested that caution must be taken when performing spectroscopic studies using techniques such as IR, NMR, XPS, and Raman, since the information derived could originate from "spectator" sulfate groups.

(4) Our study revealed the presence of a small number of zirconia crystallites containing high-Miller-index surfaces.

It was proposed that the presence of sulfate groups near or on these particles could give rise to the highly acidic sites of sulfated zirconia. The number of such catalytic sites would therefore be small.

ACKNOWLEDGMENTS

The authors are indebted to Mr. Luis Rendon for technical help and to Dr. John Higgins for helpful discussions.

REFERENCES

1. Hino, M., and Arata, K., *J. Chem. Soc. Chem. Commun.* 1148 (1979).
2. Tanabe, K., Misono, M., Yoshio, O., and Hatton, H., *in* "New Solid Acids and Bases: Their Catalytic Properties," p. 199. Elsevier, Amsterdam/Kodansha, Tokyo, 1989.
3. Yamaguchi, T., Jin, T., and Tanabe, K., *J. Phys. Chem.* **90**, 3148 (1986).
4. Hino, M., Arata, K., and Yabe, K., *Shokubai* **22**, 232 (1980).
5. Bensitel, M., Saur, O., and Lavalley, J. C., *Mater. Chem. Phys.* **19**, 147 (1988).
6. Babou, F., Coudurier, G., and Vedrine, J., *J. Catal.* **152**, 341 (1995).
7. Kustov, L. M., Kazansky, V. B., Figueras, F., and Tichit, D., *J. Catal.* **150**, 143 (1994).
8. Morterra, C., Cerrato, G., Emanuel, C., and Bolis, V., *J. Catal.* **142**, 349 (1994).
9. Nascimiento, P., Akratopoulou, C., Oszagyan, H., Coudurier, G., Travers, C., Joly, J. F., and Vedrine, J. C., *in* "Proceedings, 10th International Congress on Catalysis, Budapest, 1992." (L. Guczi, F. Solymosi, and P. Tetenyi, Eds.), p. 1185. Akadémiai Kiadó, Budapest, 1993.
10. Lunsford, J. H., Song, H., Campbell, S. M., Liang, C. H., and Anthony, R. G., *Catal. Lett.* **27**, 305 (1994).
11. Riemer, T., Spielbauer, D., Hunger, M., Mekhemer, H. A. H., and Knozinger, H., *J. Chem. Soc. Chem. Commun.* 1181 (1994).
12. Adeeva, V., de Haan, J. W., Lei, G. D., Schunemann, V., van de Ven, L. J. M., Sachtler, W. M. H., and van Santen, R. A., *J. Catal.* **151**, 364 (1995).
13. Marks, L. D., and Smith, D. J., *Nature* **303**, 316 (1983).
14. Smith, D. J., Bursill, L. A., and Jefferson, D. A., *Surf. Sci.* **175**, 673 (1986).
15. Jefferson, D. A., and Harris, P. J. F., *Nature* **332**, 617 (1988).
16. Yacamán, M. J., Herrera, R., Gómez, A., Tehuacanero, S., and Schabes, P., *Surf. Sci.* **237**, 248 (1990).
17. Parera, J. M., *Catal. Today* **15**, 481 (1992).
18. Mercera, P. D. L., Ph.D. thesis, University of Twente, 1991.
19. Somorjai, G. A., *in* "Chemistry in Two Dimensions: Surfaces," p. 157. Cornell Univ. Press, Cornell, NY, 1981.
20. Uppenbrink, J., Kirkland, A. I., Tang, D., and Jefferson, D. A., *Surf. Sci.* **238**, 132 (1990).
21. Gribelyuk, M. A., Harris, P. J. F., and Hutchison, J. L., *Phil. Mag. B* **69**, 655 (1994).